Cancer Immunology, Immunotherapy (2025) 74:154
https://doi.org/10.1007/s00262-025-04005-3

RESEARCH

Antitumor effects of immunotherapy combined with BRAF and MEK inhibitors in BRAF V600E metastatic colorectal cancer

Eunyoung Tak[1] · Hye-In An[2] · Amy Sinyoung Lee[2] · Kyuyoung Han[2] · Jiwan Choi[2] · Hyung-don Kim[3] · Yong Sang Hong[3] · Sun Young Kim[3] · Eun Kyung Choi[4] · Jeong Eun Kim[3] · Tae Won Kim[3,5]

Received: 11 July 2024 / Accepted: 26 February 2025 / Published online: 19 March 2025

Abstract

BRAF-mutated colorectal cancer correlates with poor prognosis and limited response to standard treatments. Combining immune checkpoint inhibitors with BRAF/MEK inhibitors shows promise against BRAF-mutant melanoma in both preclinical and clinical trials. Therefore, we hypothesized that the treatment would be effective against BRAF-mutant colorectal cancer. In this study, we assessed the efficacy of combining immune checkpoint inhibitors with BRAF and/or MEK inhibitors in BRAF-mutant colorectal cancers. We treated BRAF V600E colorectal cancer cells HT-29 and SNU-1235 with encorafenib (BRAF inhibitor) and binimetinib (MEK inhibitor) and assessed the degrees of MAPK inhibition, JAK/STAT inhibition, cell viability, apoptosis, and the expression of antigen presenting machinery. We also inoculated HT-29 cells into mice and treated them with an immune checkpoint inhibitor (durvalumab), encorafenib, and binimetinib for 4 weeks. We found that treatment with BRAF inhibitor, MEK inhibitor, or their combination led to significant tumor growth reduction, along with the MAPK and JAK/STAT pathway inhibition, antigen presenting machinery induction, and cytotoxic T cell activation. Our study demonstrates the potential effectiveness of combining immune checkpoint inhibitors with BRAF or MEK inhibitors for BRAF-mutated colorectal cancers.

Keywords BRAF V600E · BRAF inhibitor · MEK inhibitor · Anti-PD-L1 · Immunotherapy

Eunyoung Tak and Hye-In An have contributed equally to this work.

✉ Jeong Eun Kim
jeongeunkim@amc.seoul.kr

[1] Department of Convergence Medicine, Asan Medical Center, University of Ulsan College of Medicine, Seoul, Republic of Korea

[2] Department of Convergence Medicine, Asan Medical Institute of Convergence Science and Technology (AMIST), Asan Medical Center, University of Ulsan College of Medicine, Seoul, Republic of Korea

[3] Department of Oncology, University of Ulsan College of Medicine, 88, Olympic-Ro 43-Gil, Songpa-Gu, Seoul 05505, Republic of Korea

[4] Department of Radiation Oncology, Asan Preclinical Evaluation Center for Cancer TherapeutiX, Asan Medical Center, University of Ulsan College of Medicine, Seoul, Republic of Korea

[5] Asan Preclinical Evaluation Center for Cancer TherapeutiX, Asan Medical Center, Seoul 05505, Republic of Korea

Abbreviations

ALT	Alanine aminotransferase
AST	Aspartate aminotransferase
CRC	Colorectal cancer
IFN-γ	Interferon-gamma
ICI	Immune checkpoint inhibitors
MAPK	Mitogen-activated protein kinase
MSS	Microsatellite stable
PBMCs	Peripheral blood mononuclear cells
PD-L1	Programmed cell death ligand-1
TILs	Tumor infiltrating lymphocytes

Introduction

Colorectal cancer (CRC) is the leading cause of death worldwide and the most commonly diagnosed gastrointestinal cancer [1, 2]. Approximately 10% of CRC cases have a BRAF mutation, with the V600E mutation being the most common type. CRCs with BRAF mutations are generally associated with a poor prognosis due to an aggressive phenotype and lesser efficacy of standard cytotoxic combination

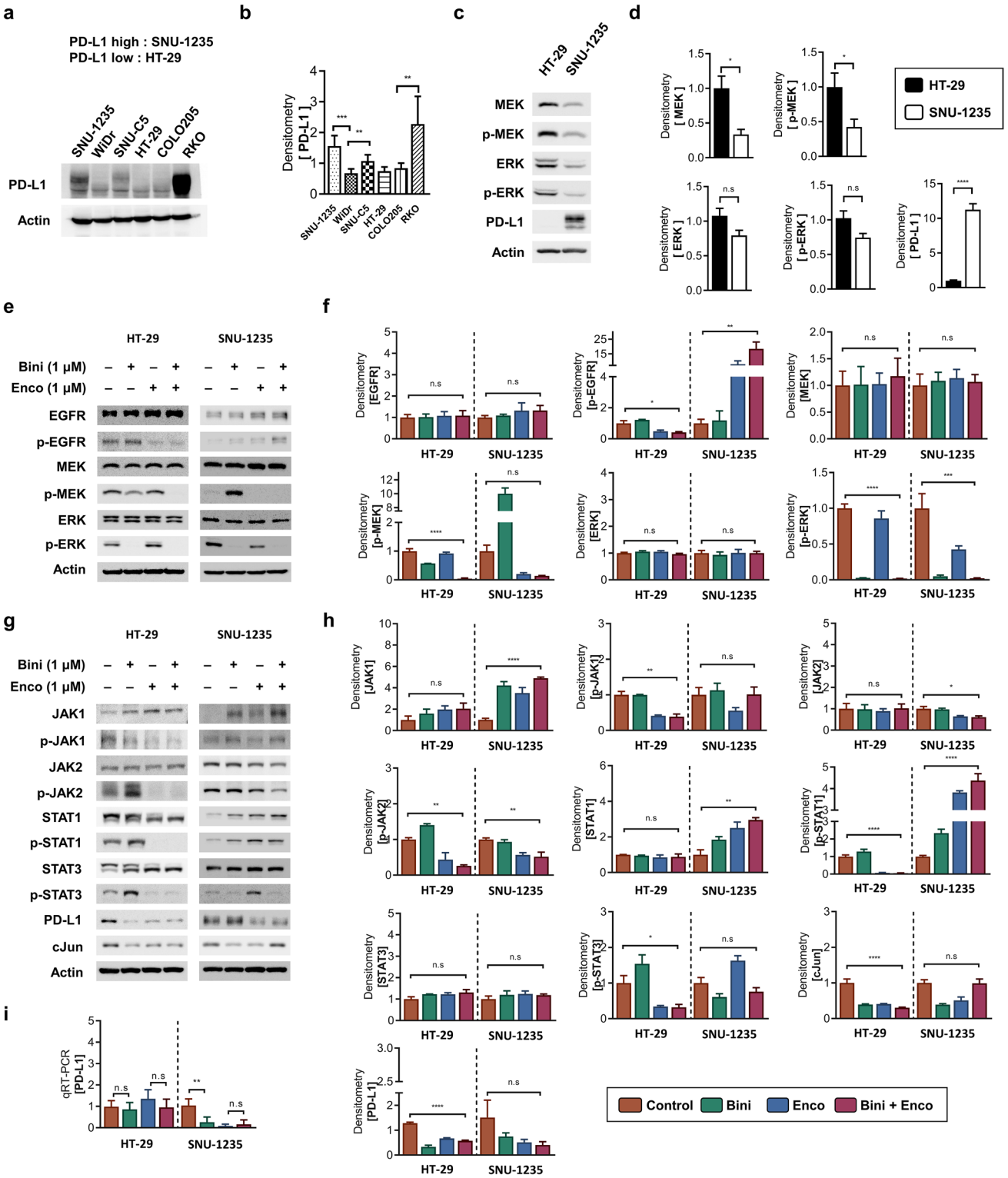

chemotherapy [3–5]. BRAF inhibitor monotherapy showed a low response rate in BRAF-mutant CRC, unlike BRAF-mutant melanoma [6–8]. Because rebound feedback after BRAF inhibition results in increased signaling through the epidermal growth factor receptor (EGFR) pathway in colon cancer [9, 10], BRAF inhibitors combined with anti-EGFR monoclonal antibodies were shown to be effective in recent studies [11–13]. Combination treatment with encorafenib (BRAF inhibitor) and cetuximab (EGFR inhibitor) has become the standard treatment for BRAF-MT CRC, following the results

◂**Fig. 1** Expression of PD-L1, MAPK and JAK/STAT pathway components in BRAF V600E colorectal cancer cell lines **a** Western blot analysis of the basal expression level of PD-L1 in BRAF V600E colorectal cancer cell lines **b** Band densitometry analysis of panel (**a**) ($n=3$) **c** Basal expression of MAPK pathway components and PD-L1 in HT-29 and SNU-1235 cell lines **d** Band densitometry analysis of panel (**c**) ($n=3$) **e** Levels of MAPK pathway component proteins in HT-29 and SNU-1235 cells treated with Binimetinib (1 μM), Encorafenib (1 μM), or both **f** Band densitometry analysis of panel (**e**) ($n=3$) **g** Levels of JAK/STAT pathway component proteins in HT-29 and SNU-1235 cells treated with Binimetinib (1 μM), Encorafenib (1 μM), or both **h** Band densitometry analysis of panel (**g**) ($n=3$) **i** mRNA level of PD-L1 in HT-29 and SNU-1235 cell lines treated with Binimetinib (1 μM), Encorafenib (1 μM), or both ($n=3$) Error bars indicate the standard error of the mean $^{*}P<0.05$, $^{**}P<0.01$, $^{***}P<0.001$, $^{****}P<0.0001$ in one-way ANOVA with Dunnett's multiple comparisons test n.s. indicates not significant Bini, Binimetinib; Enco, Encorafenib

of a phase III trial that demonstrated a significantly longer overall survival (OS) and a higher response rate compared to the previous standard therapy [14–16]. However, this regimen has a low response rate of 20%, and the response is not durable and has a short progression-free survival (PFS).

Generally, CRC shows poor response to immune checkpoint inhibitors (ICIs) such as PD-L1 inhibitors, except in cases of metastatic CRC with microsatellite instability (MSI) or mismatch repair (MMR) deficiency, in which response rates are reported to be up to 40%. In metastatic microsatellite stable (MSS) CRC, the response rate is nearly 0%. Thus, approaches to increase the immune responsiveness of MSS CRC represent a critical unmet clinical need. Approximately half of BRAF-MT CRC are classified as consensus molecular subtype 1 (CMS1), and the proportion of CMS1 is high even in MSS cases. These findings reflect an increased recognition of the immune-activated phenotype of these tumors [17]. In another study, programmed cell death ligand-1 (PD-L1) expression was shown to be associated with BRAF mutation [18]. Recent study suggested that IFN-γ-mediated upregulation of PD-L1 may be associated with poor prognosis in colorectal cancer patients by regulating JAK2/STAT1 pathway [19]. In a recent retrospective analysis, it was suggested that BRAF mutation could serve as a potential predictive biomarker for ICIs in MMR-deficient CRC with a lower response rate and shorter PFS [20].

A combination of ICI and MAPK inhibition was suggested as the strategy to enhance the antitumor efficacy in BRAF and KRAS mutant cancers [21, 22]. In addition, it was proposed that immune priming of the tumor microenvironment, through the activation of $CD8^{+}$ T cells by BRAF and/or MEK inhibitors, could be a potential mechanism of the synergistic effect [23]. Moreover, recent clinical trials in BRAF V600E melanoma showed promising efficacy and long-lasting antitumor responses with the combined inhibition of BRAF/MEK and PD-1/PD-L1 pathways [24–26]. Therefore, we assessed the antitumor effect of the triple combination of an ICI (durvalumab) and BRAF and/or MEK inhibitors in a BRAF-MT MSS CRC tumor model and delineated the underlying biological mechanisms.

Materials and methods

CRC cell lines

SNU-1235 (RRID:CVCL_5018), WiDr (RRID:CVCL_2760), SNU-C5 (RRID:CVCL_5112), HT-29 (RRID:CVCL_0320), COLO205 (RRID:CVCL_F402), and RKO (RRID:CVCL_0504) cell lines were obtained from the Korean Cell Line Bank (Seoul, Korea). These cells were cultured in RPMI-1640 (Cat #SH30027.01, Hyclone, Utah, USA) or MEM (Cat #LM 007–07, WELGENE, Gyeongsan, Korea) with 10% fetal bovine serum (Gibco, NY, USA) and 1% penicillin–streptomycin (Cat #SV30010, Hyclone, UT, USA). All of these cells were passaged for a maximum of 6 months. We confirmed the STR profile through Macrogen (Seoul, Korea) and conducted a mycoplasma assay [27].

Quantitative real-time PCR

Total RNA was collected using Qiazol lysis reagent (Qiagen) and the RNeasy mini kit (Qiagen) following a modified protocol [28]. Cells were treated with 0.5 mL of Qiazol lysis buffer, collected, and mixed with 0.1 mL of chloroform. The mixture was then centrifuged in a refrigerated centrifuge at the highest speed for 10 min. The clear supernatants were collected separately, and the nucleic acids were precipitated using 70% ethanol. The total RNAs were precipitated and bound to the silica column using the components of the RNeasy mini kit, washed twice with the RPE buffer (provided in the kit) and eluted with RNase-free distilled water (provided in the kit).

The concentration and quality of the extracted RNA were measured using Nanodrop2000 (Thermo Fisher Scientific) [29]. Samples with OD 260/280 values above 1.8 were used for experiments. The cDNA was generated from the mRNA using the ReverTra Ace qPCR RT Master Mix (Toyobo, Osaka, Japan). The transcripts were quantified using real-time reverse transcription-polymerase chain reaction (RT-PCR) with the CFX Connect Real-Time PCR Detection system (Bio-Rad, Hercules, CA, USA) and 5 × HOT FIREPol EvaGreen qPCR Supermix (Solis BioDyne, Tartu, Estonia). The samples were first denatured at 95 °C for 15 min, followed by 40 cycles of denaturation at 95 °C for 15 s, annealing at 55–60 °C for 15 s, and elongation at 72 °C for 20 s. The data are presented as the fold

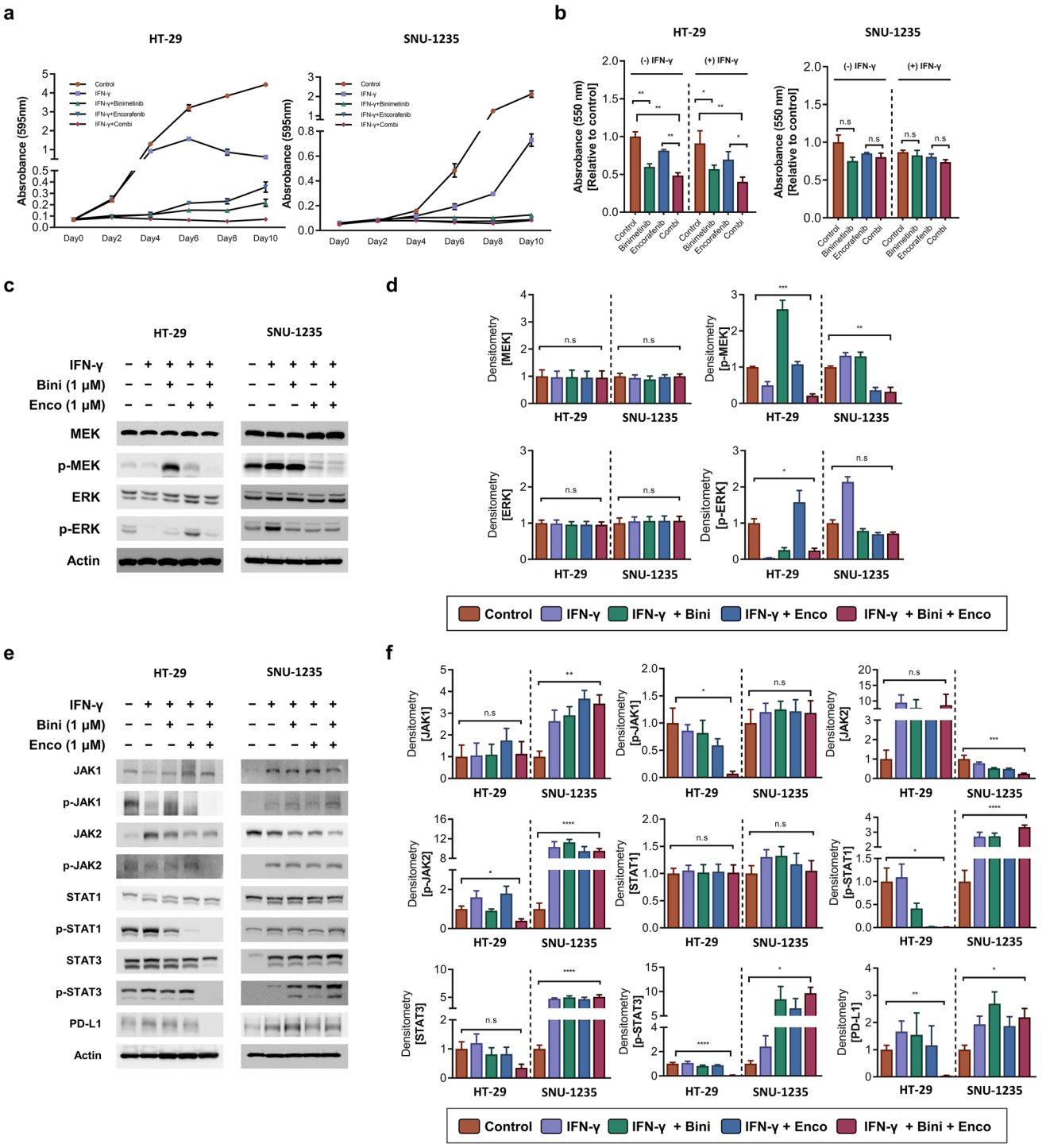

Fig. 2 Effect of Binimetinib and Encorafenib on MAPK pathway, JAK/STAT pathway and PD-L1 expression in BRAF V600E colorectal cancer cell lines in the presence of IFN-γ **a** Growth curve of HT-29 and SNU-1235 cell lines treated with the indicated combinations of IFN-γ (10 ng/ml), Binimetinib (1 μM), and Encorafenib (1 μM) for up to 10 days ($n=3$) Error bars indicate the standard deviation **b** MTT assay results of HT-29 and SNU-1235 cell lines treated Binimetinib (1 μM), Encorafenib (1 μM), or both for 48 h in the presence or absence of IFN-γ (10 ng/ml) ($n=3$) **c** Levels of MAPK pathway proteins and PD-L1 in HT-29 and SNU-1235 cell lines treated with Binimetinib (1 μM), Encorafenib (1 μM), or both in the presence of IFN-γ (10 ng/ml) (d) Band densitometry analysis of panel (**c**) ($n=3$) **e** Levels of JAK/STAT pathway proteins in HT-29 and SNU-1235 cell lines treated with Binimetinib (1 μM), Encorafenib (1 μM), or both in the presence of IFN-γ (10 ng/ml) **f** Band densitometry analysis of panel (**e**) ($n=3$) Error bars indicate the standard error of the mean $^{*}P<0.05$, $^{**}P<0.01$, $^{***}P<0.001$, $^{****}P<0.0001$ in one-way ANOVA with Dunnett's multiple comparisons test or Student's t-test n.s. indicates not significant. Bini, Binimetinib; Enco, Encorafenib

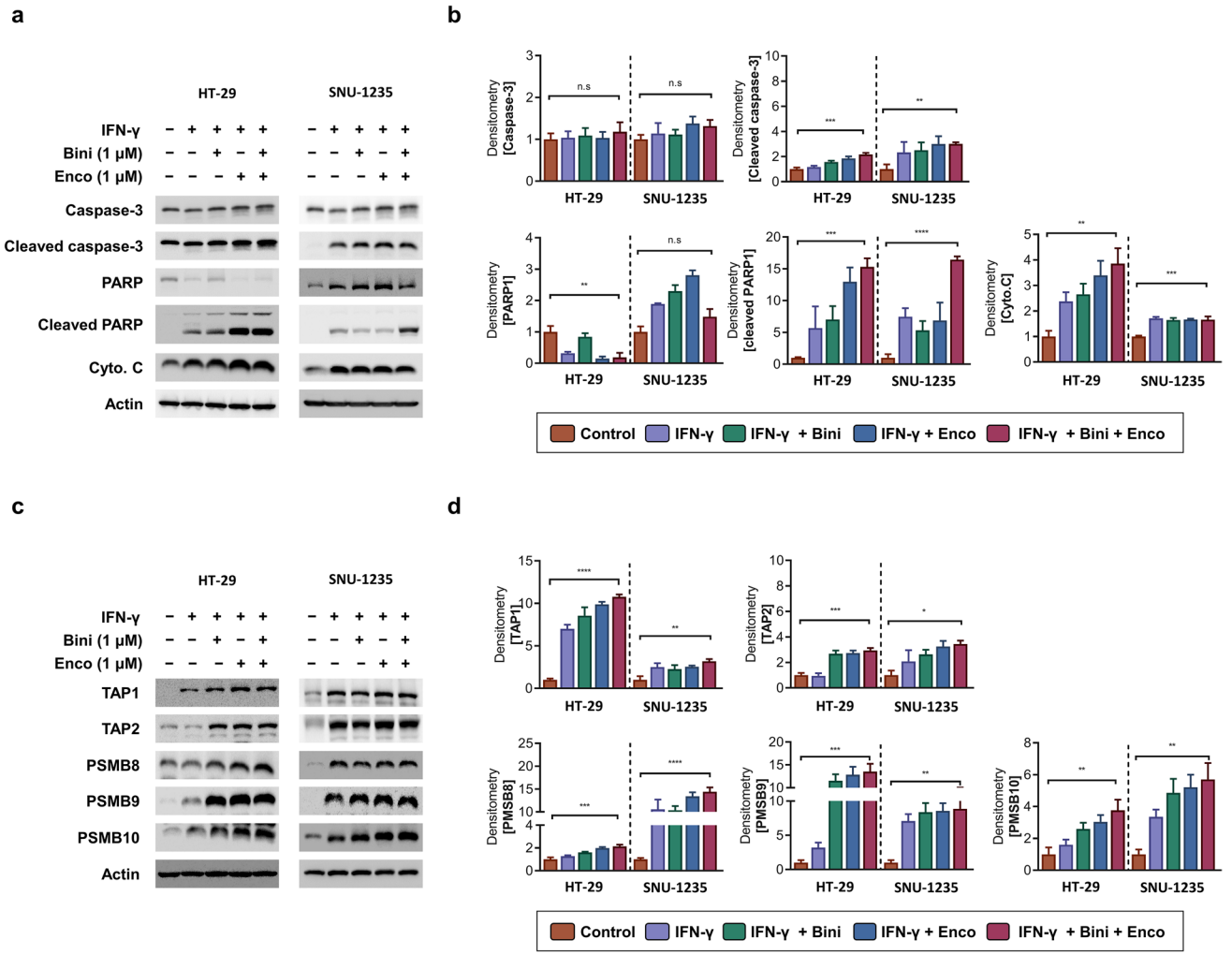

Fig. 3 Effect of Binimetinib and Encorafenib on apoptosis and immune response in BRAF V600E colorectal cancer cell lines in the presence of IFN-γ **a** Levels of apoptosis-related proteins in HT-29 and SNU-1235 cell lines treated with Binimetinib (1 μM), Encorafenib (1 μM), or both in the presence of IFN-γ (10 ng/ml) **b** Band densitometry analysis of panel (**a**) ($n=3$) **c** Levels of proteins related to antigen-presenting machinery in HT-29 and SNU-1235 cell lines treated with Binimetinib (1 μM), Encorafenib (1 μM), or both in the presence of IFN-γ (10 ng/ml) **d** Band densitometry analysis of panel (**c**) ($n=3$) Error bars indicate the standard error of the mean $*P<0.05$, $**P<0.01$, $***P<0.001$, $****P<0.0001$ in one-way ANOVA with Dunnett's multiple comparisons test or Student's t-test n.s. indicates not significant Bini, Binimetinib; Enco, Encorafenib

change in the treatment groups relative to the control and normalized to GAPDH levels.

Western blotting

For Western blotting, cells were trypsinized, washed with ice-cold PBS, and lysed in RIPA lysis buffer (50 mM HEPES [pH 7.4], 150 mM NaCl, 1 mM EDTA, 2.5 mM EGTA, 1 mM DTT, 1% Triton X-100) containing a protease and phosphatase inhibitor cocktail (Sigma). After lysis, the cell debris was removed by centrifugation at 13,000 rpm for 20 min. The protein concentrations were determined using the Bradford assay. Total cellular proteins (15 μg) were resolved by 8–15% sodium dodecyl sulfate–polyacrylamide gel electrophoresis (SDS-PAGE) and transferred to Immobilon PVDF membranes (Millipore Corporation, Billerica, MA, USA). The membranes were blocked with 5% non fat dry milk in TBST (20 mM Tris–HCl pH 7.4, 150 mM NaCl, 0.1% Tween 20) [30] and probed with anti-STAT1, anti-phospho-STAT1, anti-MEK, anti-phospho-MEK, anti-ERK, anti-phospho-ERK, anti-PD-L1, anti-TAP1, anti-TAP2, anti-PSMB8, anti-PSMB9, anti-PSMB10, anti-caspase-3, anti-c-caspase-3, anti-PARP, or anti-c-PARP, or anti-actin (Cat no. A3854, Sigma-Aldrich, St. Louis, MO, USA) primary antibodies. After washing with TBST, the primary antibodies were detected using horseradish peroxidase-conjugated

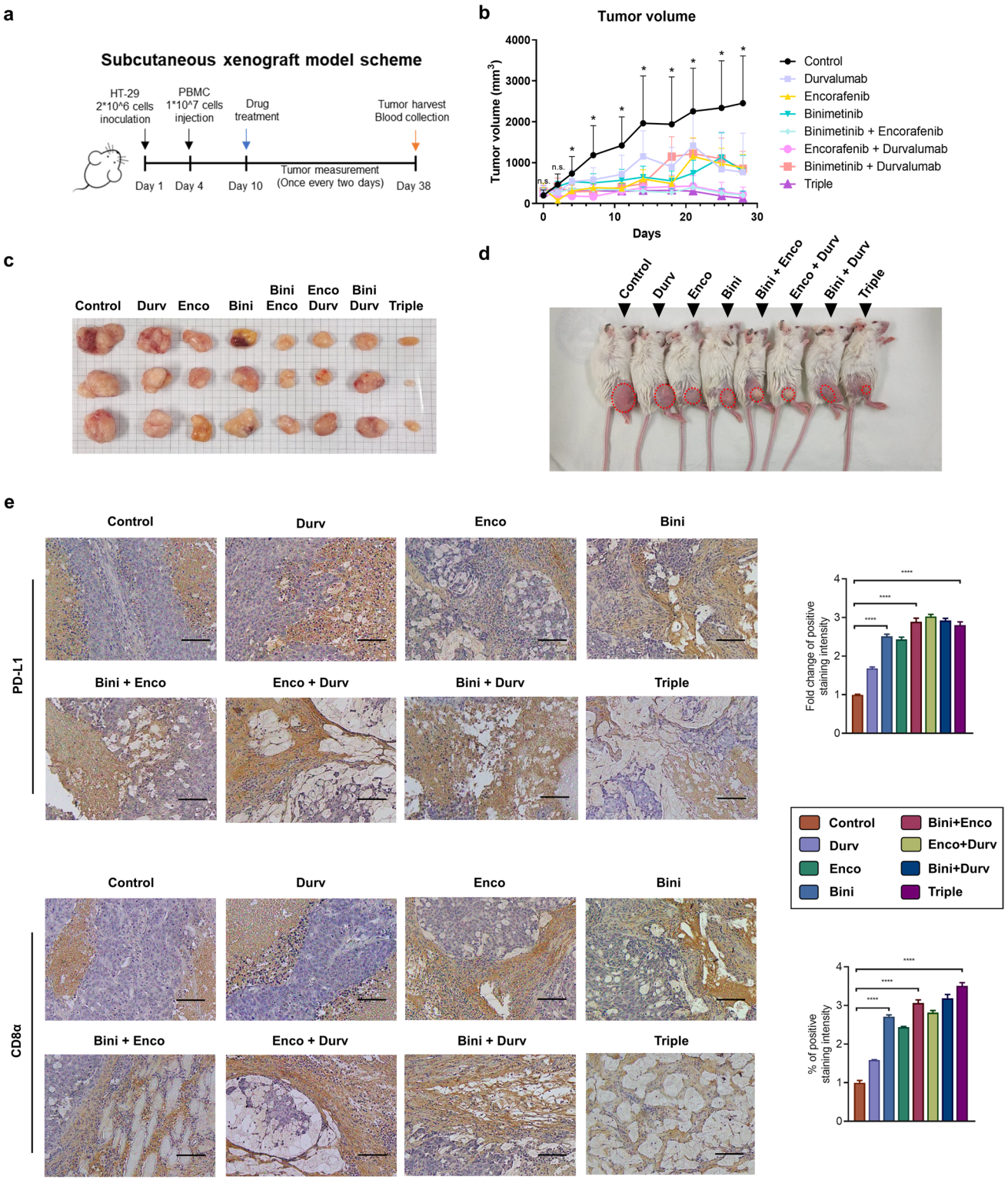

Fig. 4 Antitumor effects of the combination of immune checkpoint inhibitor and BRAF inhibitor or MEK inhibitor in vivo **a** Timeline of in vivo experiments **b** Tumor growth curve in xenograft mice (Control group, $n=20$; Drug-treated groups, $n=18$) **c** Gross image of tumors harvested from xenograft mice **d** Gross image of mice 4 weeks after drug treatment **e** Immunohistochemistry results of PD-L1 and CD8α in the tumor tissues Scale bar, 100 μm ($n=3$) Error bars denote the standard error of the mean $^*P<0.001$ in one-way ANOVA with Dunnett's multiple comparisons test n.s. indicates not significant Bini, Binimetinib; Enco, Encorafenib; Durv, Durvalumab

goat-rabbit secondary antibodies and an enhanced chemiluminescence detection system (Amersham, Buckinghamshire, UK).

Flow cytometric analysis

We isolated tumor-infiltrating lymphocytes (TILs) from the tumor tissues of NRG mice humanized with PBMCs (Tumor Dissociation kit, Human, Miltenyi Biotec). To stain the surface of the cells [31], Brilliant Stain Buffer (Cat. No 566349, BD HorizonTM) and antibodies were incubated on ice for 18 min: PerCP-Cy™5.5 Mouse Anti-Human CD45 (Cat. no. 564105, BD Pharmingen™), BV786 Mouse Anti-Human CD4 (Cat. no. 563877, BD Horizon™), Alexa Fluor® 700 Mouse Anti-Human CD8 (Cat. no. 557945, BD Pharmingen™), Brilliant Violet 421™ anti- human CD279 (PD-1) Antibody (Cat. no 329920, BioLegend), PE-CF594 Mouse Anti-Human HLA-DR (Cat. no. 562304, BD Horizon™), Brilliant Violet 650™ anti-human CD38 Antibody (Cat No. 356620, BioLegend), CD39 Monoclonal Antibody (eBioA1 (A1)), FITC, eBioscience™ (Cat. no. 11–0399-42, Invitrogen™). After washing with PBS, fixation was performed with eBioscience™ FOXP3/Transcription Factor Staining Buffer Set (Cat. no. 00–5523-00, Invitrogen™) for intracellular staining, followed by incubation on ice for 18 min. After washing with Permeabilization Buffer in FOXP3/Transcription Factor Staining Buffer Set, intracellular staining antibody was added and incubated for 20 min at room temperature: Brilliant Violet 605™ anti-human Ki-67 Antibody (Cat. no. 350522, BioLegend), FOXP3 Monoclonal Antibody (PCH101), PE, eBioscience™ (Cat. no. 12–4776-42, Invitrogen™). We performed flow cytometry analysis (CytoFLEX, BECKMAN COULTER) the following day after washing with Permeabilization Buffer overnight at 4 °C. Cells were classified as live or dead by the LIVE/DEAD™ Fixable Near-IR Dead Cell Stain Kit for 633 or 635 nm excitation (Cat. no. L34976, Invitrogen™). FlowJo software (Tree Star) was used to analyze the data.

Xenograft model and in vivo experiments

Animal care procedures and experiments received approval from the Institutional Animal Care and Use Committee (IACUC) at Asan Medical Center (AMC). NRG mice were allocated into one control group ($n = 20$) and seven experimental groups ($n = 18$) following the approved protocols. The NRG mice aged 8 weeks were used (Cat. no. GEM-0006, JA BIO). HT-29 cells were subcutaneously injected into mice at a concentration of $2 \times 10\text{^}6$ cells/mouse. Three days after injection, $1 \times 10\text{^}7$ cells/mouse of human peripheral blood mononuclear cells (PBMCs, Zen bio) were treated with DNase I (Sigma Aldrich) 1 mg/mL to construct a PBMC humanized mouse model via tail vein injection, reflecting the human immune system. From 7 days after PBMC injection, encorafenib (HY-15605, MedChemExpress) 5 mg/kg, binimetinib (HY-15202, MedChemExpress) 3 mg/kg daily, and durvalumab (AstraZeneca) 10 mg/kg were administered orally twice a week for 4 weeks. Twice a week, the tumor volume was measured using the following formula: major axis × minor axis^2 × 0.52. After 28 days of drug treatment, we harvested tumor samples. Durvalumab was generously provided by AstraZeneca (Cambridge, UK) for research purposes.

Serum measurement assays

Whole-blood samples were obtained from the inferior vena cava of the mice and coagulated in serum separator tubes (SSTs; Becton Dickinson and Company). The SST tubes were incubated for 30 min at room temperature (22 ± 2 °C) and then centrifuged at 2500 × g for 20 min at 4 °C. The supernatants were collected and stored as serum samples. Serum alanine aminotransferase (ALT) and aspartate aminotransferase (AST) levels were analyzed by a Hitachi 7180 autoanalyzer (Tokyo, Japan).

Histological analysis and immunohistochemistry

Liver tissues were resected, fixed in 4% formalin, and embedded in paraffin. The paraffin blocks were sectioned with a microtome to produce 4 μm-thick sections. To assess the severity of liver injury, the H&E-stained slides were scored using Suzuki's method with historical criteria for the assessment of liver damage after severe ischemia and reperfusion injury based on the presence and severity of sinusoidal congestion, cytoplasmic vacuolization, and necrosis of parenchymal cells by a pathologist. For immunohistochemistry (IHC), the sections were deparaffinized in xylene, rehydrated using an alcohol gradient, boiled in 10 mM citrate buffer (pH 6.0) for 20 min to retrieve antigens, and then treated with 0.3% hydrogen peroxide in methanol.

Cell proliferation assay

Cells were seeded on a 24-well plate with 5000 cells per well. Cells were fixed in 10% formalin and stained with 0.1% crystal violet at the indicated intervals. We measured the optical density at 595 nm after extracting the dye with 10% acetic acid.

Statistical analysis

Data are presented as mean ± standard error of the mean from three to eight samples per condition. Statistical analyses were performed using either the Student's t-test (two

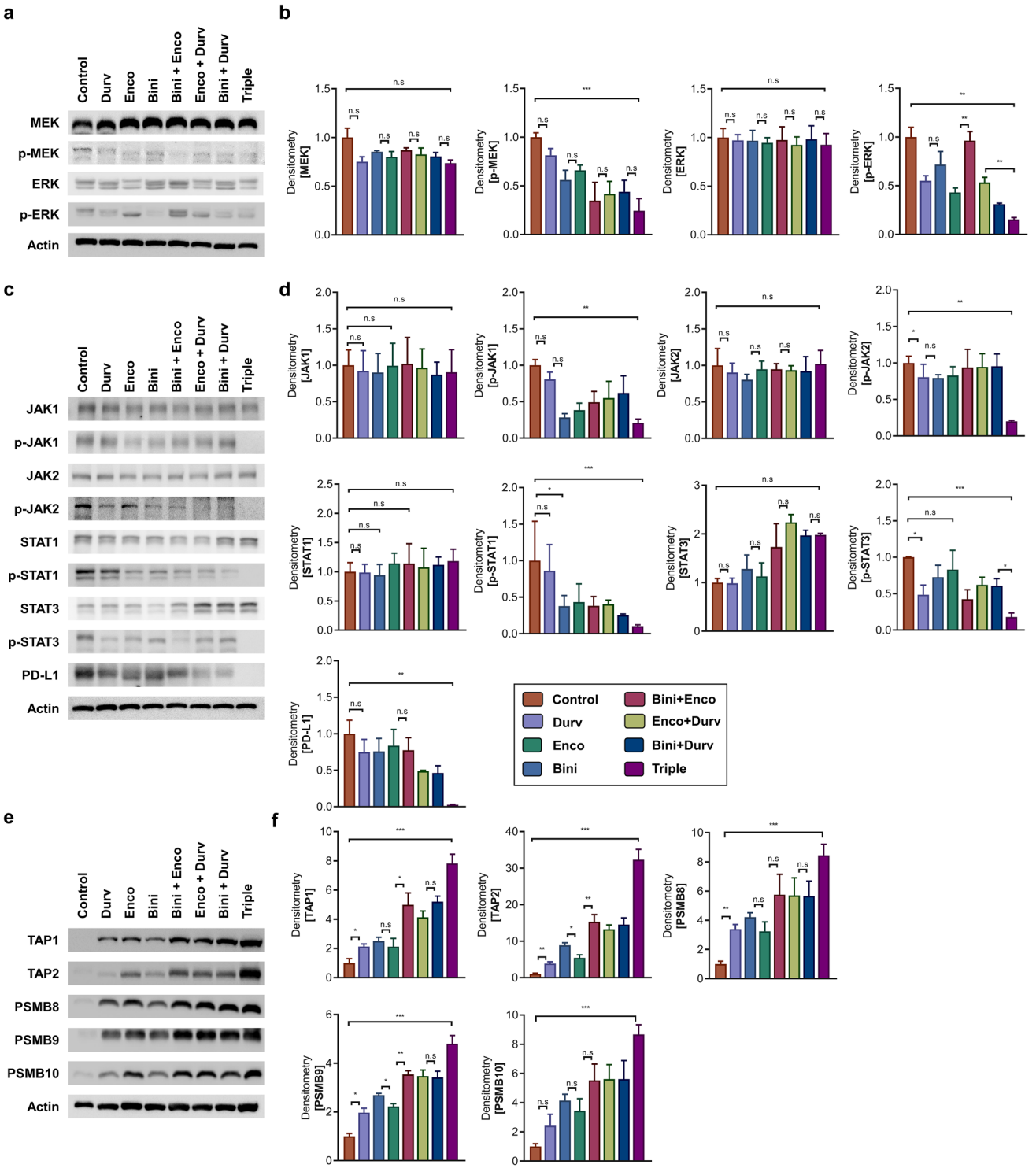

Fig. 5 Effect of combination of immune checkpoint inhibitor and BRAF inhibitor or MEK inhibitor on MAPK pathway, JAK/STAT pathway and antigen-presenting machinery in vivo **a** Western blot analysis of MAPK pathway component proteins in the tumors of xenograft mice treated with an immune checkpoint inhibitor (anti-PD-L1; Durvalumab, 10 mg/kg), Binimetinib (3 mg/kg), Encorafenib (5 mg/kg), or their indicated combinations **b** Band densitometry analysis of panel (**a**) ($n=3$) **c** Western blot analysis of JAK/STAT pathway component and PD-L1 in the tumors of xenograft mice after indicated drug treatment **d** Band densitometry analysis of panel (**c**) ($n=3$) **e** Western blot analysis of the proteins involved in the antigen-presenting machinery in the tumors of xenograft mice after indicated drug treatment **f** Band densitometry analysis of panel (**e**) ($n=3$) Error bars indicate the standard error of the mean $^{*}P<0.05$, $^{**}P<0.01$, $^{***}P<0.001$, $^{****}P<0.0001$ in one-way ANOVA with Dunnett's multiple comparisons test or Student's t-test n.s. indicates not significant Bini, Bini; Enco, Enco; Durv, Durvalumab

samples, equal variance) or the one-way ANOVA (multiple experimental groups, one factor) for two experimental groups [32]. A statistically significant value was defined as $p < 0.05$. Western blotting was performed three times. For all statistical analysis, we used the Stata 15.1 software (College Station, TX, USA) and the GraphPad Prism 7.0 software (College Station, TX, USA).

RESULTS

Expression pattern of PD-L1, MAPK and JAK/STAT pathway inhibition in BRAF V600E colorectal cancer cell lines

We first assessed the basal protein expression level of PD-L1 in BRAF V600E colorectal cancer cell lines (Fig. 1a, b). Among these cell lines, cell lines with a high expression of PD-L1 (SNU-1235) and a low expression of PD-L1 (HT-29) were selected, and assessed the basal levels of MAPK pathway components and PD-L1 (Fig. 1c, d). We then examined the changes in those proteins after treatment with binimetinib (MEK inhibitor) or encorafenib (BRAF inhibitor) (Fig. 1e, f), and found that the combination treatment of binimetinib and encorafenib resulted in the highest degree of MAPK pathway inhibition in HT-29. In contrast, in SNU-1235 cells, combination treatment of binimetinib and encorafenib reduced the levels of p-MEK and p-ERK while not resulting in significant differences in p-EGFR and c-Jun. Also, we investigated PD-L1 expression level after combination treatment. As a result, JAK/STAT pathway was inhibited which also led to down regulation of PD-L1 expression only in HT-29 (Fig. 1g, h).

qRT-PCR analysis showed that while the mRNA level of PD-L1 was not significantly changed in response to treatment with binimetinib, encorafenib, or both, the same was significantly reduced in SNU-1235 when treated with both binimetinib and encorafenib (Fig. 1i).

Binimetinib and encorafenib treatment reduces the viability of BRAF V600E colorectal cancer cell lines

For viability measurement, we treated the cell lines with IFN-γ to consider the surrounding immune environment. In the presence of IFN-γ, the treatment of binimetinib, encorafenib, or their combination resulted in a significant inhibition in cell growth (Fig. 2a). MTT assay showed that regardless of the presence of IFN-γ, treatment with binimetinib, encorafenib, or their combination resulted in a significant reduction of cell viability; in contrast, SNU-1235 cells did not show significant reductions in cell viability in response to drug treatment, regardless of the presence of IFN-γ (Fig. 2b).

We then assessed the changes in the expression levels of proteins involved in the MAPK pathway in HT-29 and SNU-1235 cell lines in the presence of IFN-γ (Fig. 2c, d). Treatment with binimetinib and encorafenib led to significant alterations in the phosphorylated forms of MAPK pathway proteins (p-MEK, p-ERK) in HT-29 cells but not in SNU-1235 cells.

Also, we examined JAK/STAT pathway in HT-29 and SNU-1235 in the presence of INF- γ. The expression level of JAK/STAT pathway components and PD-L1 was significantly reduced in HT-29 cells but increased in SNU-1235 cells in response to combination treatment with binimetinib and encorafenib (Fig. 2e, f).

Binimetinib and encorafenib treatment enhance apoptosis and immune responses in BRAF V600E colorectal cancer cell lines

In terms of apoptosis, Western blot analysis on caspase-3, PARP, and cytochrome C showed that the combination treatment resulted in the highest degree of apoptosis in both HT-29 and SNU-1235 cell lines (Fig. 3a, b). We also found that in both HT-29 and SNU-1235 cell lines, combination treatment led to significant increases in the levels of proteins involved in the antigen-presenting machinery, which plays a crucial role in cancer immunotherapy (Fig. 3c, d).

Co-administration of binimetinib, encorafenib, and anti-PD-L1 shows a significant synergistic effect in vivo

We then confirmed the in vitro effect of binimetinib and encorafenib in vivo using a xenograft model. First, HT-29 cells ($2 \times 10\text{^}6$ cells) were subcutaneously injected into humanized NRG mice. After 3 days, human PBMCs ($1 \times 10\text{^}7$ cells) were injected into the tail vein, and drug administration began 7 days later. In this experiment, the mice were administered binimetinib (3 mg/kg daily), encorafenib (5 mg/kg daily), durvalumab (10 mg/kg twice a week), or their combinations (binimetinib + encorafenib, binimetinib + durvalumab, encorafenib + durvalumab, or triple [binimetinib + encorafenib + durvalumab]). Tumor volume and body weight were measured twice a week, and mice were sacrificed 28 days after drug treatment (Fig. 4a, Supplementary Fig. 1).

While all drug-treated groups showed a reduction in tumor growth compared with the vehicle-treated control group, the triple-treated group showed the greatest degree of reduction in tumor growth (Fig. 4b, c, and d, $P < 0.001$). There was no statistically significant difference in mouse body weight changes between the control group and the

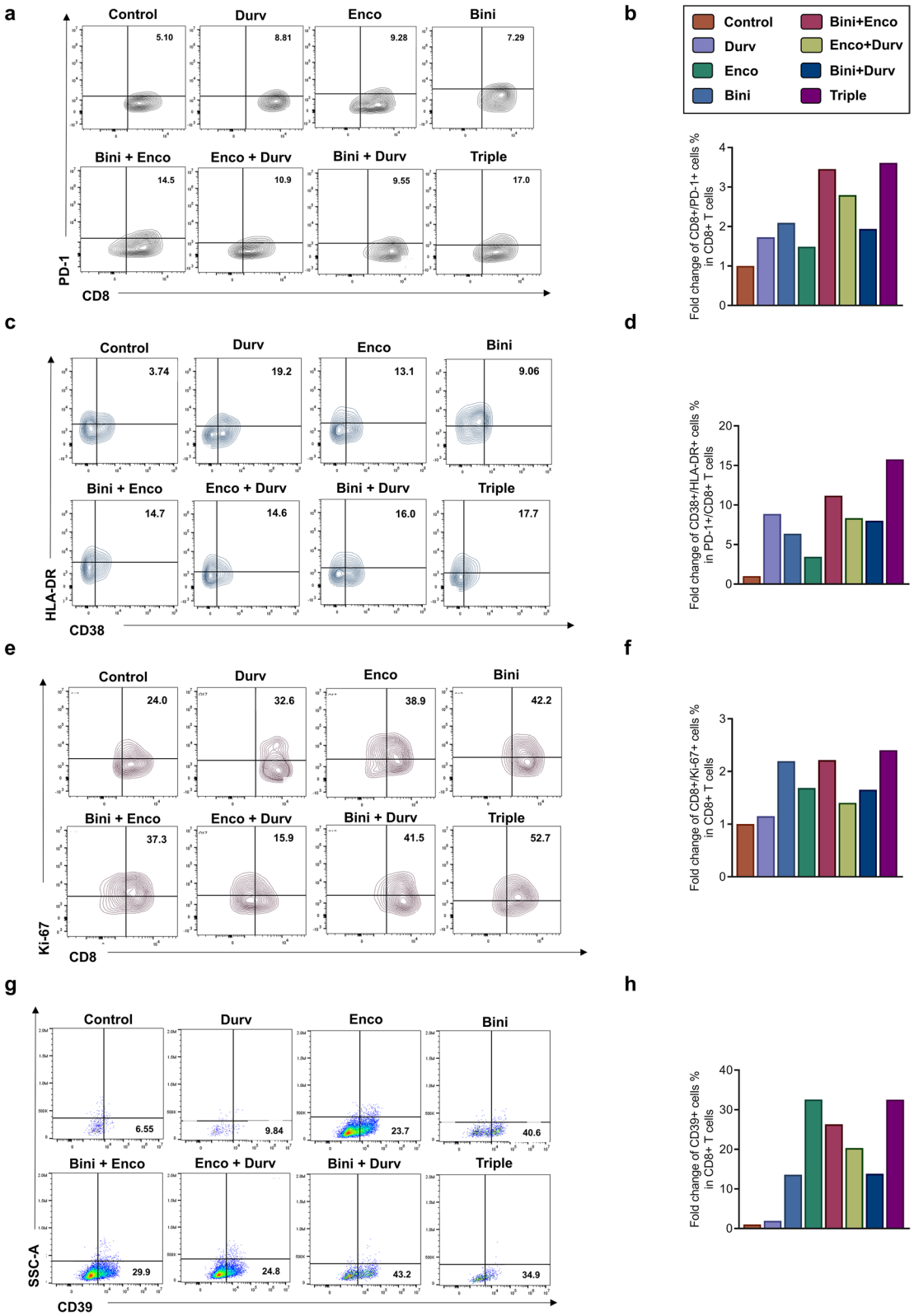
a
Control
Durv
Enco
Bini
5.10
8.81
9.28
7.29
Bini + Enco
Enco + Durv
Bini + Durv
Triple
14.5
10.9
9.55
17.0
PD-1
CD8
b
Control
Durv
Enco
Bini
Bini+Enco
Enco+Durv
Bini+Durv
Triple
Fold change of CD8+/PD-1+ cells % in CD8+ T cells
c
Control
Durv
Enco
Bini
3.74
19.2
13.1
9.06
Bini + Enco
Enco + Durv
Bini + Durv
Triple
14.7
14.6
16.0
17.7
HLA-DR
CD38
d
Fold change of CD38+/HLA-DR+ cells % in PD-1+/CD8+ T cells
e
Control
Durv
Enco
Bini
24.0
32.6
38.9
42.2
Bini + Enco
Enco + Durv
Bini + Durv
Triple
37.3
15.9
41.5
52.7
Ki-67
CD8
f
Fold change of CD8+/Ki-67+ cells % in CD8+ T cells
g
Control
Durv
Enco
Bini
6.55
9.84
23.7
40.6
Bini + Enco
Enco + Durv
Bini + Durv
Triple
29.9
24.8
43.2
34.9
SSC-A
CD39
h
Fold change of CD39+ cells % in CD8+ T cells

◂**Fig. 6** Activation of CD8 + T cells in response to the combination of immune checkpoint inhibitor and BRAF inhibitor or MEK inhibitor FACS analysis was performed on the tumor tissues of xenograft mice treated with an immune checkpoint inhibitor (anti-PD-L1; Durvalumab, 10 mg/kg), Binimetinib (3 mg/kg), Encorafenib (5 mg/kg), or their indicated combinations **a** Gating results for PD-1 and CD8 **b** Proportion of CD8 + /PD-1 + cells among CD8 + cells **c** Gating results for HLA-DR and CD38 **d** Proportion of CD38 + /HLA-DR + cells among PD-1 + /CD8 + cells **e** Gating results for Ki-67 and CD8 **f** Proportion of CD8 + /Ki-67 + cells among CD8 + cells **g** Gating results for CD39 **h** Proportion of CD39 + cells among CD8 + cells Bini, Bini; Enco, Enco; Durv, Durvalumab

drug-treated group (Supplementary Fig. 1). After the completion of all drug treatments, we examined Liver H&E and measured AST and ALT levels for drug toxicity assessment. There was no difference between the control group and the drug treat group, so it was confirmed that there was no drug toxicity (Supplementary Fig. 3a). AST and ALT levels did not show a difference between the control group and the drug treat group or showed a tendency to decrease, confirming that there is no drug toxicity (Supplementary Fig. 3b).

We also performed immunohistochemistry for PD-L1 and CD8α to assess the changes in the antigen-presenting machinery and the degree of necrosis in the implanted tumors. We found that the levels of PD-L1 and CD8α both increased in the tumors in response to treatment with binimetinib, encorafenib, and durvalumab; moreover, we observed that the degree of necrosis was higher in the drug-treated groups as well (Fig. 4e).

Triple treatment leads to MAPK inhibition, JAK/STAT inhibition and an increase in antigen-presenting machinery proteins in vivo

We then assessed the degree of MAPK inhibition in the xenograft model. In agreement with the in vitro results, the degree of MAPK inhibition was the most pronounced in the triple-treatment group, as evidenced by the decreases in p-MEK and p-ERK (Fig. 5a, b). Interestingly, the level of p-ERK was significantly higher in the binimetinib + encorafenib group compared with the binimetinib alone group.

Next, we investigated the inhibition pattern of the JAK/STAT pathway. Results confirmed that the phosphorylated form was mostly downregulated in the triple treatment group. Consequently, the expression of PD-L1 also exhibited the most substantial decrease in the triple treatment group (Fig. 5c, d). We also observed that the proteins involved in the antigen-presenting machinery increased in the drug-treated groups, especially the triple-treatment group, likely owing to activations in T cells (Fig. 5e, f).

T cell activation in tumor-infiltrating lymphocytes in response to triple-treatment

Previous studies reported that tumor infiltration of lymphocytes does not occur in MSS colorectal cancer and that the level of tumor-infiltrating lymphocytes (TILs) correlates with the response to ICIs [33]. We therefore performed a flow cytometry analysis of TILs to assess whether $CD8^+$ T cells are activated in the drug-treated xenograft models. In our study, we performed TIL isolation by pooling tumor tissues from each group. First, we investigated the proportion of human lymphocytes within the total TIL population. The proportion of human lymphocytes was highest in the binimetinib + durvalumab treated group among all the groups (Supplementary Fig. 2a, b). Next, as we explored the distribution of CD4 and CD8 T cells, we observed a consistent pattern of increasing proportions associated with drug treatment administration (Supplementary Fig. 2c–e). Similarly, the distribution of Regulatory T cells showed an increasing trend in the groups treated with the drug (Supplementary Fig. 2f, g). Then we assessed the expression level of PD-1 as a T cell activation marker in $CD8^+$ T cells and found that the greatest degree of PD-1 expression was found in the triple-treatment group (Fig. 6a). The proportion of PD-1^+ cells among $CD8^+$ cells was also higher in the triple-treatment group compared to the control group (Fig. 6b). We then assessed the proportions of HLA-DR^+ and $CD38^+$ cells among the $CD8^+$/PD-1^+ T cells to further assess the degree of T cell activation (Fig. 6c). As expected, the proportion of HLA-DR^+/$CD38^+$ double-positive cells was the highest in the triple-treatment group (Fig. 6d). Similar results were obtained for the proportion of Ki-67^+ cells (Fig. 6e, f) and $CD39^+$ cells (Fig. 6g, h) among $CD8^+$ T cells.

Discussion

In this study, we demonstrated the improved antitumor activity of an ICI (durvalumab) combined with a MEK inhibitor (binimetinib) and/or a BRAF inhibitor (encorafenib) in BRAF-MT MSS CRC cell lines and a BRAF-MT MSS CRC humice xenograft model. Treatment of these drugs, especially triple-treatment, led to increases in antitumor activity obtained via the activation of T cells in TILs, as well as increases in the expression of antigen-presenting machinery proteins. Specifically, combining two therapies (BRAF inhibitor, MEK inhibitor) led to an increase in the proportion of proliferative and tumor-specific $CD8^+$/PD-1^+ T cells, as well as increased activation of $CD8^+$/PD-1^+ T cells.

Previous studies on BRAF mutant melanoma have shown that MAPK inhibition [34]and BRAF inhibitors can elevate PD-L1 expression, increase antigen expression, and promote the infiltration of CD8-positive T lymphocytes into tumors

[35–38]. Building on these findings, combining BRAF inhibition with ICI has been shown to enhance response and prolong survival in both a preclinical mouse model of BRAF mutant melanoma [39–41] and in patients with BRAF mutant melanoma [24–26, 42, 43]. Another study revealed that BRAF-MT CRC is characterized by an immune microenvironment with high expression levels of several immunotherapeutic targets, including PD-1, PD-L1, CTLA-5, LAG-C, and TIM-3[44]. Furthermore, patients with BRAF-MT CRC who exhibit complement activation and an increase in M2 macrophages in their tumor microenvironment tend to have a poorer prognosis [45]. Given this evidence, it is suggested that combining ICIs with BRAF inhibitors could significantly enhance treatment efficacy for BRAF-MT CRCs.

To replicate the human CRC model in the HT-29 cell line, we treated the cells with IFN-γ and conducted in vitro experiments. Our study suggests that the combined use of ICIs, along with BRAF and/or MEK inhibitors, can potentially mitigate the risk of BRAF-MT CRC by promoting immune-related alterations in the tumor microenvironment. This treatment activated T cells and induced the expression of antigen-presenting machinery proteins. A phase 2 trial has previously demonstrated the effectiveness of a similar combination in treating BRAF-MT CRC patients undergoing chemotherapy [46]. Also, the study reported a 25% response rate for ICIs combined with MEK and BRAF inhibitors in BRAF-MT CRC patients. These patients had a median progression-free survival rate of 5 months. The same study also revealed, through single-cell RNA sequencing of 23 paired pre-treatment and on-treatment biopsies, that a stronger induction of tumor cell-intrinsic immune programs and complete MAPK inhibition correlated with improved clinical outcomes. However, that study did not assess the tumor microenvironment since their primary focus was on the tumor cell component, leaving the status of T cell activation and changes in antigen-presenting machinery proteins unexplored. This is a distinction from our research, where we evaluated these factors.

Our study has certain limitations that should be acknowledged. The efficacy of our combined treatment approach in relation to the tumor microenvironment needs further exploration. In our in vitro experiments, we demonstrated the effectiveness of this combined strategy in treating solid tumors, specifically using the BRAF-MT MSS CRC cell line. Further studies are needed to confirm the potential of this combined approach.

The limited availability of BRAF-MT MSS CRC cell lines led us to utilize only one cell line for our in vivo model study. The generalizability of our results would be enhanced by using a broader range of cell lines, especially those derived from patients, in subsequent studies. Through flow cytometry, we observed the presence of immune cells in the tumor microenvironment. However, compared to cutting-edge methods like single-cell genomics, epigenomics, and in-situ multiplex immunohistochemistry techniques, flow cytometry offers limited insights into potential mechanisms tied to novel treatment strategies.

Nevertheless, our research has shown that the combination of ICI with BRAF and/or MEK inhibitors can activate T cells in tumor-infiltrating lymphocytes. This lends support to the notion that such a combined approach is an effective treatment for patients with BRAF-MT CRC. A strength of our study lies in demonstrating the efficacy of ICIs when combined with BRAF and/or MEK inhibitors, without the need for a monoclonal anti-EGFR antibody, in a straightforward humanized mouse model of BRAF-MT MSS CRC. Furthermore, our findings pave the way for the development of innovative strategies to enhance the survival of patients diagnosed with BRAF-MT CRC, particularly by pairing ICI and BRAF inhibitors to optimize treatment outcomes.

Supplementary Information The online version contains supplementary material available at https://doi.org/10.1007/s00262-025-04005-3.

Author contributions JEK and ET conceptualized the study, designed the experiments, interpreted the data, and wrote the manuscript; HA conducted the experiments, analyzed and interpreted the data, and made the figures; AL and KH conducted some experiments, analyzed and interpreted the data; HK and JC analyzed/interpreted the data and reviewed the manuscript; YH and EC provided patients samples and reviewed the manuscript, SK identified and characterized the treatment protocol; TK provided technical and conceptual support on studies.

Funding This research was supported by the National Research Foundation of Korea (NRF) grant (grant number 2020R1G1A1099822), the Bio & Medical Technology Development Program of the NRF (grant number 2017M3A9B6061825) funded by the Korean government, Ministry of Science and ICR (MSIT) and Health Technology R&D Project through the Korea Health Industry Development Institute (KHIDI), funded by the Ministry of Health & Welfare, Republic of Korea (grant number HI20C1586, RS-2018-KH049509 and RS-2023-00261982).

Data availability No datasets were generated or analysed during the current study.

Declarations

Competing interests The authors declare no competing interests.

Ethics approval This study was approved by the Institutional Animal Care and Use Committee (IACUC) at Asan Medical Center (AMC) (Approval number 2021–12-022).

References

1. Arnold M, Abnet CC, Neale RE, Vignat J, Giovannucci EL, McGlynn KA, Bray F (2020) Global burden of 5 major types of gastrointestinal cancer. Gastroenterology 159:335–49.e15. https://doi.org/10.1053/j.gastro.2020.02.068
2. Hong S, Won YJ, Park YR, Jung KW, Kong HJ, Lee ES (2020) Cancer statistics in Korea: incidence, mortality, survival, and prevalence in 2017. Cancer Res Treat 52:335–350. https://doi.org/10.4143/crt.2020.206
3. Kayhanian H, Goode E, Sclafani F et al (2018) Treatment and survival outcome of BRAF-mutated metastatic colorectal cancer: a retrospective matched case-control study. Clin Colorectal Cancer 17:e69–e76. https://doi.org/10.1016/j.clcc.2017.10.006
4. Tran B, Kopetz S, Tie J et al (2011) Impact of BRAF mutation and microsatellite instability on the pattern of metastatic spread and prognosis in metastatic colorectal cancer. Cancer 117:4623–4632. https://doi.org/10.1002/cncr.26086
5. Morris V, Overman MJ, Jiang Z-Q et al (2014) Progression-free survival remains poor over sequential lines of systemic therapy in patients with BRAF-mutated colorectal cancer. Clin Colorectal Cancer 13:164–171. https://doi.org/10.1016/j.clcc.2014.06.001
6. Kopetz S, Desai J, Chan E et al (2015) Phase II pilot study of vemurafenib in patients with metastatic braf-mutated colorectal cancer. J Clin Oncol 33:4032–4038. https://doi.org/10.1200/jco.2015.63.2497
7. Seligmann JF, Fisher D, Smith CG et al (2017) Investigating the poor outcomes of BRAF-mutant advanced colorectal cancer: analysis from 2530 patients in randomised clinical trials. Ann Oncol 28:562–568. https://doi.org/10.1093/annonc/mdw645
8. Hyman DM, Puzanov I, Subbiah V et al (2015) Vemurafenib in multiple nonmelanoma cancers with BRAF V600 mutations. N Engl J Med 373:726–736. https://doi.org/10.1056/NEJMoa1502309
9. Prahallad A, Sun C, Huang S, Di Nicolantonio F, Salazar R, Zecchin D, Beijersbergen RL, Bardelli A, Bernards R (2012) Unresponsiveness of colon cancer to BRAF(V600E) inhibition through feedback activation of EGFR. Nature 483:100–103. https://doi.org/10.1038/nature10868
10. Corcoran RB, Ebi H, Turke AB et al (2012) EGFR-mediated re-activation of MAPK signaling contributes to insensitivity of BRAF mutant colorectal cancers to RAF inhibition with vemurafenib. Cancer Discov 2:227–235. https://doi.org/10.1158/2159-8290.Cd-11-0341
11. Corcoran RB, André T, Atreya CE et al (2018) Combined BRAF, EGFR, and MEK inhibition in patients with BRAF(V600E)-mutant colorectal cancer. Cancer Discov 8:428–443. https://doi.org/10.1158/2159-8290.Cd-17-1226
12. Kopetz S, Guthrie KA, Morris VK et al (2021) Randomized trial of irinotecan and cetuximab with or without vemurafenib in BRAF-mutant metastatic colorectal cancer (SWOG S1406). J Clin Oncol. https://doi.org/10.1200/Jco.20.01994
13. Hong DS, Morris VK, El Osta B et al (2016) Phase IB study of vemurafenib in combination with irinotecan and cetuximab in patients with metastatic colorectal cancer with BRAFV600E mutation. Cancer Discov 6:1352–1365. https://doi.org/10.1158/2159-8290.CD-16-0050
14. Kopetz S, Grothey A, Yaeger R et al (2019) Encorafenib, binimetinib, and cetuximab in BRAF V600E–mutated colorectal cancer. N Engl J Med 381:1632–1643. https://doi.org/10.1056/NEJMoa1908075
15. Tabernero J, Grothey A, Van Cutsem E et al (2021) Encorafenib plus cetuximab as a new standard of care for previously treated BRAF V600E-mutant metastatic colorectal cancer: updated survival results and subgroup analyses from the BEACON study. J Clin Oncol 39:273–284. https://doi.org/10.1200/jco.20.02088
16. van Geel R, Tabernero J, Elez E et al (2017) A phase Ib dose-escalation study of encorafenib and cetuximab with or without alpelisib in metastatic BRAF-mutant colorectal cancer. Cancer Discov 7:610–619. https://doi.org/10.1158/2159-8290.Cd-16-0795
17. Guinney J, Dienstmann R, Wang X et al (2015) The consensus molecular subtypes of colorectal cancer. Nat Med 21:1350–1356. https://doi.org/10.1038/nm.3967
18. Rosenbaum MW, Bledsoe JR, Morales-Oyarvide V, Huynh TG, Mino-Kenudson M (2016) PD-L1 expression in colorectal cancer is associated with microsatellite instability, BRAF mutation, medullary morphology and cytotoxic tumor-infiltrating lymphocytes. Mod Pathol 29:1104–1112. https://doi.org/10.1038/modpathol.2016.95
19. Zhao T, Li Y, Zhang J, Zhang B (2020) PD-L1 expression increased by IFN-gamma via JAK2-STAT1 signaling and predicts a poor survival in colorectal cancer. Oncol Lett 20:1127–1134. https://doi.org/10.3892/ol.2020.11647
20. Sahin IH, Goyal S, Pumpalova Y et al (2021) Mismatch repair (MMR) gene alteration and BRAF V600E mutation are potential predictive biomarkers of immune checkpoint inhibitors in mmr-deficient colorectal cancer. Oncologist 26:668–675. https://doi.org/10.1002/onco.13741
21. Ebert PJR, Cheung J, Yang Y et al (2016) MAP kinase inhibition promotes T Cell and anti-tumor activity in combination with PD-L1 checkpoint blockade. Immunity 44:609–621. https://doi.org/10.1016/j.immuni.2016.01.024
22. Hong A, Piva M, Liu S et al (2021) Durable suppression of acquired MEK inhibitor resistance in cancer by sequestering MEK from ERK and promoting antitumor T-cell immunity. Cancer Discov 11:714–735. https://doi.org/10.1158/2159-8290.CD-20-0873
23. Liu L, Mayes PA, Eastman S et al (2015) The BRAF and MEK inhibitors dabrafenib and trametinib: effects on immune function and in combination with immunomodulatory antibodies targeting PD-1, PD-L1, and CTLA-4. Clin Cancer Res 21:1639–1651. https://doi.org/10.1158/1078-0432.CCR-14-2339
24. Dummer R, Lebbe C, Atkinson V et al (2020) Combined PD-1, BRAF and MEK inhibition in advanced BRAF-mutant melanoma: safety run-in and biomarker cohorts of COMBI-i. Nat Med 26:1557–1563. https://doi.org/10.1038/s41591-020-1082-2
25. Ribas A, Lawrence D, Atkinson V et al (2019) Combined BRAF and MEK inhibition with PD-1 blockade immunotherapy in BRAF-mutant melanoma. Nat Med 25:936–940. https://doi.org/10.1038/s41591-019-0476-5
26. Sullivan RJ, Hamid O, Gonzalez R et al (2019) Atezolizumab plus cobimetinib and vemurafenib in BRAF-mutated melanoma patients. Nat Med 25:929–935. https://doi.org/10.1038/s41591-019-0474-7
27. Tak E, Kim M, Cho Y et al (2022) Expression of neurofibromin 1 in colorectal cancer and cetuximab resistance. Oncol Rep. https://doi.org/10.3892/or.2021.8226
28. Koh WU, Kim J, Lee J, Song GW, Hwang GS, Tak E, Song JG (2019) Remote ischemic preconditioning and diazoxide protect

from hepatic ischemic reperfusion injury by inhibiting HMGB1-induced TLR4/MyD88/NF-kappaB signaling. Int J Mol Sci. https://doi.org/10.3390/ijms20235899
29. Kwon JH, Lee J, Kim J et al (2019) HIF-1alpha regulates A2B adenosine receptor expression in liver cancer cells. Exp Ther Med 18:4231–4240. https://doi.org/10.3892/etm.2019.8081
30. Tak E, Park GC, Kim SH, Jun DY, Lee J, Hwang S, Song GW, Lee SG (2016) Epigallocatechin-3-gallate protects against hepatic ischaemia-reperfusion injury by reducing oxidative stress and apoptotic cell death. J Int Med Res 44:1248–1262. https://doi.org/10.1177/0300060516662735
31. Lee J, Choi J, Kang S et al (2020) Hepatogenic potential and liver regeneration effect of human liver-derived mesenchymal-like stem cells. Cells. https://doi.org/10.3390/cells9061521
32. Kwon JH, Lee J, Kim J et al (2019) Upregulation of carbonyl reductase 1 by Nrf2 as a potential therapeutic intervention for ischemia/ reperfusion injury during liver transplantation. Mol Cells 42:672–685. https://doi.org/10.14348/molcells.2019.0003
33. Bai Z, Zhou Y, Ye Z, Xiong J, Lan H, Wang F (2021) Tumor-infiltrating lymphocytes in colorectal cancer: the fundamental indication and application on immunotherapy. Front Immunol 12:808964. https://doi.org/10.3389/fimmu.2021.808964
34. Dankner M, Lajoie M, Moldoveanu D et al (2018) Dual MAPK inhibition is an effective therapeutic strategy for a subset of class II BRAF mutant melanomas. Clin Cancer Res 24:6483–6494. https://doi.org/10.1158/1078-0432.Ccr-17-3384
35. Frederick DT, Piris A, Cogdill AP et al (2013) BRAF inhibition is associated with enhanced melanoma antigen expression and a more favorable tumor microenvironment in patients with metastatic melanoma. Clin Cancer Res 19:1225–1231. https://doi.org/10.1158/1078-0432.Ccr-12-1630
36. Liu C, Peng W, Xu C et al (2013) BRAF inhibition increases tumor infiltration by T cells and enhances the antitumor activity of adoptive immunotherapy in mice. Clin Cancer Res 19:393–403. https://doi.org/10.1158/1078-0432.Ccr-12-1626
37. Hu-Lieskovan S, Mok S, Moreno BH et al (2015) Improved antitumor activity of immunotherapy with BRAF and MEK inhibitors in BRAF(V600E) melanoma. Sci Transl Med. https://doi.org/10.1126/scitranslmed.aaa4691
38. Peiffer L, Farahpour F, Sriram A et al (2021) BRAF and MEK inhibition in melanoma patients enables reprogramming of tumor infiltrating lymphocytes. Cancer Immunol Immunother 70:1635–1647. https://doi.org/10.1007/s00262-020-02804-4
39. Cooper ZA, Juneja VR, Sage PT et al (2014) Response to BRAF inhibition in melanoma is enhanced when combined with immune checkpoint blockade. Cancer Immunol Res 2:643–654. https://doi.org/10.1158/2326-6066.CIR-13-0215
40. Lelliott EJ, McArthur GA, Oliaro J, Sheppard KE (2021) Immunomodulatory effects of BRAF, MEK, and CDK4/6 inhibitors: implications for combining targeted therapy and immune checkpoint blockade for the treatment of melanoma. Front Immunol 12:661737. https://doi.org/10.3389/fimmu.2021.661737
41. Lai X, Friedman A (2017) Combination therapy for melanoma with BRAF/MEK inhibitor and immune checkpoint inhibitor: a mathematical model. BMC Syst Biol 11:70. https://doi.org/10.1186/s12918-017-0446-9
42. Welti M, Dimitriou F, Gutzmer R, Dummer R (2022) Triple combination of immune checkpoint inhibitors and BRAF/MEK inhibitors in BRAFV600 melanoma: current status and future perspectives. Cancers. https://doi.org/10.3390/cancers14225489
43. Liu Y, Zhang X, Wang G, Cui X (2021) Triple combination therapy With PD-1/PD-L1, BRAF, and MEK inhibitor for stage III-IV melanoma: a systematic review and meta-analysis. Front Oncol 11:693655. https://doi.org/10.3389/fonc.2021.693655
44. Cen S, Liu K, Zheng Y, Shan J, Jing C, Gao J, Pan H, Bai Z, Liu Z (2021) BRAF mutation as a potential therapeutic target for checkpoint inhibitors: a comprehensive analysis of immune microenvironment in BRAF mutated colon cancer. Front Cell Dev Biol. https://doi.org/10.3389/fcell.2021.705060
45. Kim JE, Kim J-H, Kim S-Y, Cho H, Ryu Y-M, Hong YS, Kim SY, Kim TW (2022) Immune profile of BRAF-mutated metastatic colorectal tumors with good prognosis after palliative chemotherapy. Cancers 14:2383
46. Tian J, Chen JH, Chao SX et al (2023) Combined PD-1, BRAF and MEK inhibition in BRAFV600E colorectal cancer: a phase 2 trial. Nat Med 29:458–466. https://doi.org/10.1038/s41591-022-02181-8